Proceedings of the 18th INDIACom; INDIACom-2024; IEEE Conference ID: 61295
2024 11th International Conference on "Computing for Sustainable Global Development", 28th Feb. – 1st Mar., 2024
Bharati Vidyapeeth's Institute of Computer Applications and Management (BVICAM), New Delhi (INDIA)

Diabetes Mellitus Diagnosis using Optical Ring Resonators

Manush Prajwal
Dept. Computer Science and Engineering
The Oxford College of Engineering
Bangalore, India
manushprajwal555@gmail.com

J Jesy Janet Kumari
Dept. Computer Science and Engineering
The Oxford College of Engineering
Bangalore, India
ebijesy.j@gmail.com

Maanas Mitrahass Uppu
Dept. Computer Science and Engineering
The Oxford College of Engineering
Bangalore, India
maanasmitrahass@gmail.com

Vanajaroselin Chirchi
Dept. of ISC
The Oxford College of Engineering
Bangalore, India
vr.chirchi@gmail.com

S Vishalatchi
Dept. of ECE
Kalasalingam Academy of Research and Education
Krishnankoil, India
vishalisks@gmail.com

Darshan D N
Dept. Computer Science and Engineering
The Oxford College of Engineering
Bangalore, India
darshandn2555@gmail.com

***Abstract*- The research shows the use of optical ring resonators (ORRs) as a promising non-invasive tool for diagnosing diabetes mellitus, potentially replacing invasive procedures. By accurately measuring glucose levels in biological samples through resonance frequency shifts closely linked to varying glucose concentrations, ORRs point to innovative and precise glucose measurement for early diabetes detection. This advancement could transform disease monitoring by reducing patient discomfort from current invasive techniques. The study develops a highly sensitive, non-invasive method for detecting diabetes by analyzing subtle optical signal changes related to glucose levels in urine is around 165-180 mg/dl (normal) and resonant frequency output is around 36.026459 but in case of blood resonant frequency output is around0.348478amusing advanced optical ring resonator technology. The methodology involves designing optical ring resonators capable of detecting minute refractive index variations connected to glucose concentrations. Major findings demonstrate the precision of diagnosing diabetes, showcasing the potential for a rapid and reliable diagnostic tool. Interpretations emphasize the innovative approach's ability to significantly improve early detection, enabling timely intervention and enhanced diabetes management for better healthcare outcomes and quality of life for individuals with diabetes.**

Keywords— ring resonator, diabetes mellitus, diabetes diagnosis, non-invasive method, optical signal.

I. Introduction

Diabetes mellitus is a chronic metabolic disorder characterized by elevated blood glucose levels resulting from insufficient or ineffective insulin production or use. It might lead to problems with the heart, kidneys, eyes, and nerves. Genetic susceptibility and lifestyle factors impact its development; treatment options include medication, diet, and exercise. Hyperglycemia, or increased blood sugar, is one of the key markers of diabetes mellitus [1], a chronic metabolic disorder caused by either inadequate insulin synthesis or insufficient insulin absorption by the body. The pancreas secretes the hormone insulin, which controls how much glucose cells can absorb and use as fuel. Diabetes mellitus is caused by a disruption in this control. Diabetes Mellitus Causes: Environmental factors and genetic predisposition are the main causes [2]. The immune system accidentally targets and destroys the beta cells in the pancreas that produce insulin, leading to type 1 diabetes. The most prevalent kind of diabetes, type 2, is frequently linked to obesity, sedentary lifestyles, and poor eating habits—all of which increase insulin resistance [3] and decrease insulin production. During a fast, normal blood glucose levels normally fall between 70 and 99 mg/dL. Within this range, normal urine glucose levels also occur.

Blood sugar levels may rise momentarily after eating, but they normally return to normal in a few hours. Over time, high blood sugar may lead to problems. Urine from a healthy person has no glucose. However, excess glucose leaks into the urine and is referred to as glucosuria [4] when blood glucose levels surpass the kidney's threshold for reabsorption, which is around 180 mg/dL . The main issue is the need for a quick, accurate, and non-invasive diabetic testing procedure. A plasmonic silicon-on-insulator ring resonator biosensor is used in this work. Refractive index fluctuations, surface plasmon polaritons, and waveguide coupling are examples of specific terminologies. The goal is to maximize the sensitivity of the sensor to astonishingly small variations in refractive index that correspond to concentrations of glucose in urine [5]. The goal of the study is to assess the sensor's performance with exceptional resolution throughout a certain range of refractive indices. Real-time detection and improved sensitivity are made possible by the optimal field confinement in the sensor area.

The ability of this biosensor to detect increased amounts in urine has potential for a number of medical applications, such as the early diagnosis of diabetes and the identification of conditions linked to abnormal glucose metabolism. The ultimate objective is to integrate this reliable biosensor into point-of-care instruments, influencing diabetes diagnosis approaches and strategies with enhanced diagnostic effectiveness and accessibility

II. Literature Review

An architecture is created with a silicon non-insulator (SOI) ring resonator arrangement. The single waveguide structure and the double waveguide structure in Figure.2 are combined into a ring with an outside radius of the ring as indicated in Figure 1 [6]. The device's design makes use of parametric optimization approach and modal analysis. [7]. Ridge waveguide is the term for the 400 nm wide, Si-based material (nsi=3.477) straight waveguide.

The width of the Si ridge wave guide is 200 nm, and the ring width is 20 nm. The distance between the ridge and the ring is 60 nm. The ring (Fig. 1) wafer initial dimensions are 8 nm in length and 6 nm in breadth. Diagram illustrating the plasmonic ring resonator

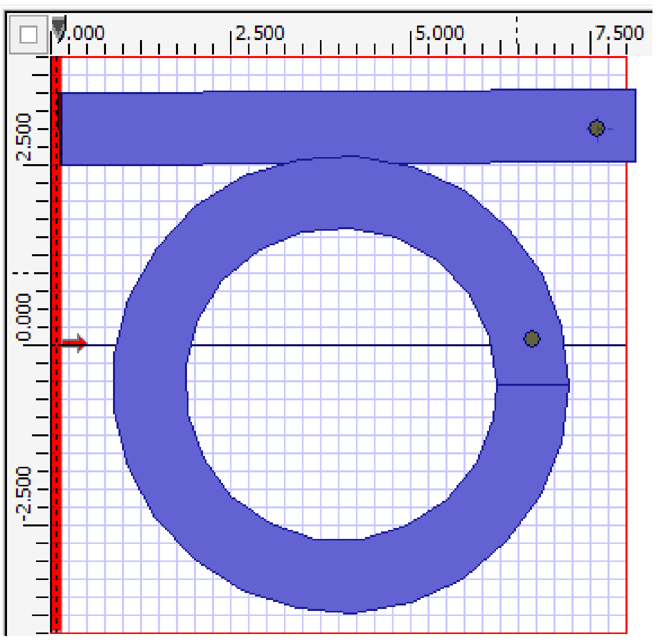

Fig. 1. Image of single waveguide of ring resonator in 2D plain

For a wavelength of 1.4 nm, all of the previously given refractive index values are taken into account [8]. The structure's cross-sectional image shows the 2.5 nm cladding thickness. With these dimensions, the waveguide's depth is 220 nm. This is the area where the maximum confinement is seen.Consequentlythere is a maximum chance of an electric field interaction [9]. Permittivity always has opposing signs (+,-) at the Plasmon's excitation surface of the dielectric-metal interface.Internal reflection of p-polarized light is the source of resonant Plasmon wave excitation [10]. One notable benefit of using surface plasmon resonance (SPR) in biosensing is that it can improve electric field confinement at the contact [11]. Enhancing the Interaction of incident light [12] enhances the sensitivity. Low blood glucose concentrations (40–60 mg/dl) are the first signs of "hypoglycemia" [13], and urine's refractive index drops from 1.335 to 1.2 [14]. The transmission spectrums for hypoglycemic and normal urine have already been studied by authors [15], who have already focused on low blood glucose concentrations. In MEEP units, the peak transmission frequency and transmitted output power for normal urine are 0.375050100200396 [16]. and 36.0264596534466 [17]., respectively, whereas for hypoglycemic urine they are 0.400901803607209 and 85.2123400793049.[18].

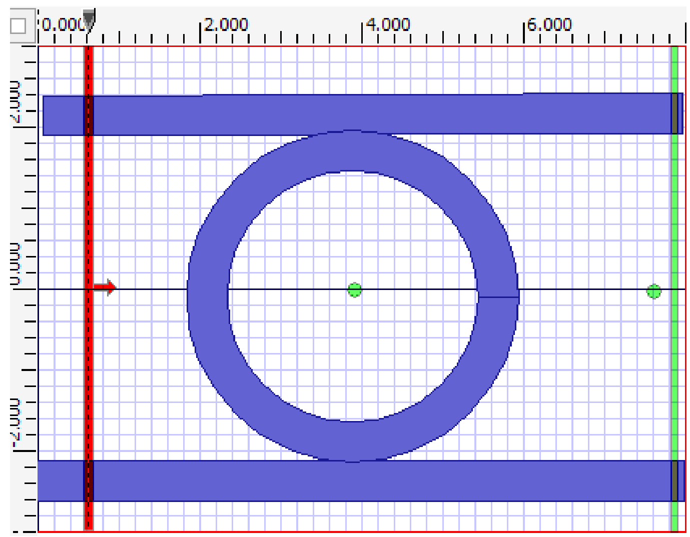

Fig. 2. Image of double waveguide of ring resonator in 2D plain

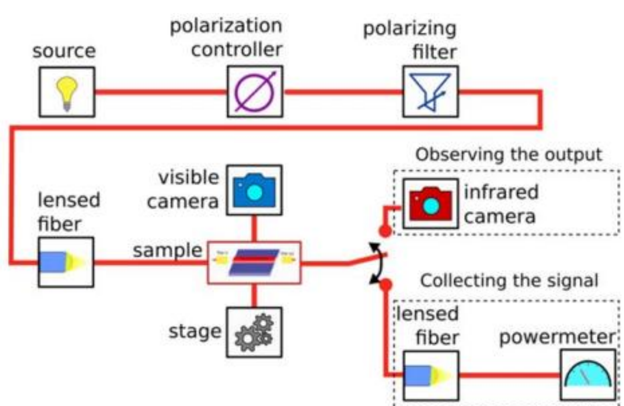

Fig. 3. Proposed Model

Step 1: Supply of Light

The light source is an intense pulsed laser beam. The optical fiber is connected to the laser beam.

Step 2: The Optical Fiber's Propagation

Via the optical fiber, the light pulse travels. Light interacts with the molecules in the fiber's core as it travels.

Step 3: Interaction with the Molecules Glucose

In the fiber'scenter, the glucose molecules are in contact with the light pulse. The light pulse's strength drops as a result of the glucose molecules' partial absorption of light.

Step 4: Getting Out of the Fiber Optic

The optical cable releases the pulse of light. A detector measures the pulse's intensity of light.

Step 5: Signal Processing: A PC processes the signal that comes from the detector. The amount of light that the glucose molecules absorbed is calculated by the computer.

Step 6: Determine Your Blood Glucose Concentration

To determine the blood glucose concentration, one uses the quantity of light absorbed by the glucose molecules

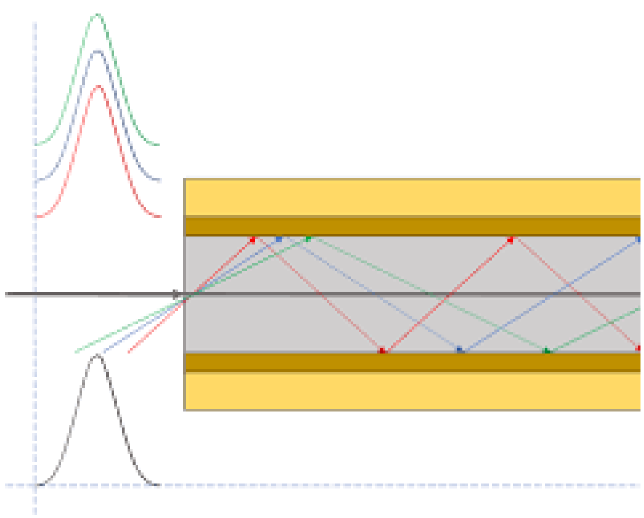

Fig. 4. Transmission of light rays through optical fiber

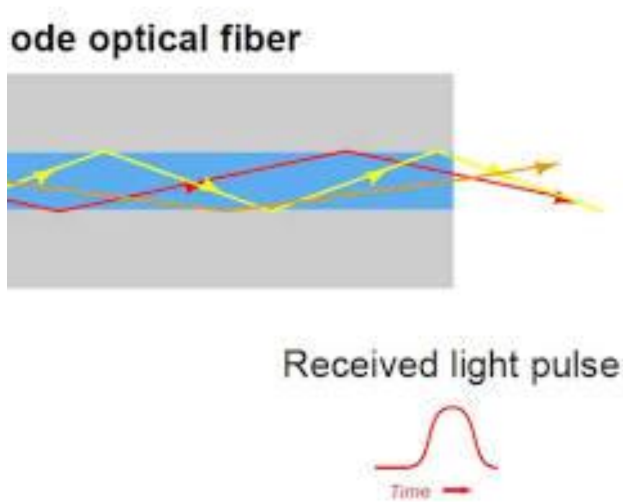

Fig. 5. Transmission of light rays through optical fiber

The recommended system's main steps are as follows:

1) A pulsed laser beam serves as the light source.

2) The light pulse is propagated by the optical fiber.

3) The light pulse interacts with the glucose molecules located in the center of the fiber.

4) The light pulse exits the optical wire at this point.

5) The strength of the light pulse is measured by a detector.

6) The signal from the detector is processed by a computer.

7) The computer calculates how much light is absorbed by the glucose molecules.

8) Measuring the amount of light received by the glucose molecules yields the blood glucose concentrationThis is a new and perhaps useful method of diagnosing diabetes mellitus.

III. Proposed System and Implementation

To test the refractive index biosensor's sensing ability, we used is 1.4 nm wavelength range with 0.1 nm resolution. The sensor was originally optimized for air cladding, producing four resonant peaks that met the resonance wavelength requirements for an optical ring resonator structure, as described in [19],[20].

$$2\pi rnef = m\lambda m \quad (1)$$

The resonance wavelength λm of the ring resonator depends on the ring radius r, effective refractive index neff, and integer mode order m. At 1561.4 nm, the resonant wavelength exhibited resonant peaks in power propagation [21] through the ring resonator. The photonic crystal structure acts as an optical insulator that blocks light transmission within certain frequency ranges, demonstrated by plotting the photonic band gap versus wave vector k [22]. Introducing defects into the photonic crystal waveguide manipulates the band gap, controlling light flow for potential sensing applications [23]. Light propagation in the waveguide obeys Maxwell's equations, described by Equation (2):

$$\nabla \times (1 \in \nabla \times H) = (\omega C) 2 H \quad (2)$$

In this equation, the dielectric function (ε), which is equal to η2 (where η is the refractive index), and frequency (ω) have an inverse connection. ε stands for permittivity.

Utilizing the Finite Difference Time Domain (FDTD) approach, the Massachusetts Institute of Technology developed the Electromagnetic Equation Propagation (MEEP) modeling tool [24]. The time-dependent curl equations of Maxwell are directly solved using this numerical analytic method to simulate electromagnetic (EM) fields. It functions by using Equations (3) and (4) to represent the sampling of the continuous electromagnetic field at discrete locations in time and space (within a defined volume).

$$\partial f/\partial x\ (iAx,,jAy,\ kAz) = (f''\ (i + 1/2, j, k) - f''\ (i + 1/2, j,k))/\Delta x + o[(At) \quad (3)$$

$$\partial f\ /\partial x\ (\ (iAx,\ jAy,\ kAz) = (fn+1/2\ (i,\ j,k)\ —\ fn-1/2\ (i,\ j,\ k))/\Delta t + o[(At) \quad (4)$$

An iterative procedure that updates the field values at each grid point based on Maxwell's curl equations in finite difference form is used to compute the transmission flux after an excitable Gaussian pulse with sinusoidal modulation excites the structure [25]. Until a stable state is reached, the iterative process is continued. To calculate the transmission flux in designated locations, MEEP then solves for P(t), the time-dependent Poynting vector. As indicated by Equation [26], the frequency domain response P(ω) is obtained via Fourier transform of the time domain flux data P(t)[27].

$$:P(\omega) = \mathrm{Re}\ \hat{n}\ .\ E\omega(x) * \times H\omega(x)\ d2x \qquad (5)$$

The directional energy flow, or power per unit area, of an electromagnetic field is represented by the Poynting vector. In this case, the power density is computed using the real component of the dot product between the unit vector and the complex Poynting vector in the propagation direction. Next, the outcome is integrated across the volume.

TABLE I. GLUCOSE CONCENTRATION IN BLOOD VARIATIONS IN INPUT AND TRANSMITTED OUTPUT POWER IN CASE OF DIABETES MELLITUS [28]

Blood sample containing varying glucose concentrations (mg/d 1)	**Changes in blood glucose content that result in fluctuations in the urine's refractive index.**	**Peak Transmission (in Meep units)**	**Power of Transmitted Output (in Meep units)**
165-180 (normal)	1.335	0.3750501	36.026459
182	1.337	0.3750501	36.0117104
205	1.338	0.3750501	35.420536
220	1.338	0.3750501	35.420536
240	1.338	0.3750501	35.420536
255	1.338	0.3750501	35.420536
289	1.338	0.3750501	35.420536
342	1.339	0.3744489	35.285957

TABLE II. REFRACTIVE INDICES USED FOR THE SENSOR FOR THE DETECTION OF DIABETES MELLITUS IN BLOOD

Blood sample with varying glucose concentrations in milligrams per day (mg/d 1)	**Fluctuation in the blood glucose concentration that results in changes in the urine's input refractive index.**	**Resonant frequency of output**
165-180 (normal)	1.335	0.348478
182	1.337	0.348435
205	1.338	0.348413
220	1.338	0.348413
240	1.338	0.348413
255	1.338	0.348413
289	1.338	0.348413
342	1.339	0.348392

IV. RESULTS

Plotted the shift in wavelength for increase in refractive index as shown in Fig. 6. Plotted the shift in wavelength for increase in refractive index Power spectrum graph for single waveguide: Graph for Fig. 7. Power loss as in Fig. 8.Power spectrum graph for double waveguide is as shown in Fig. 9.

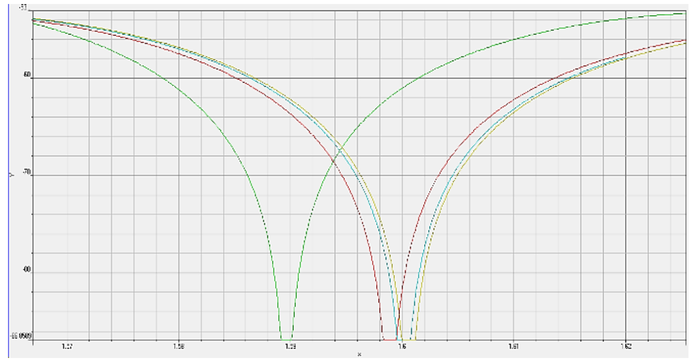

Fig. 6. Relative power vs. distance graph for double waveguide

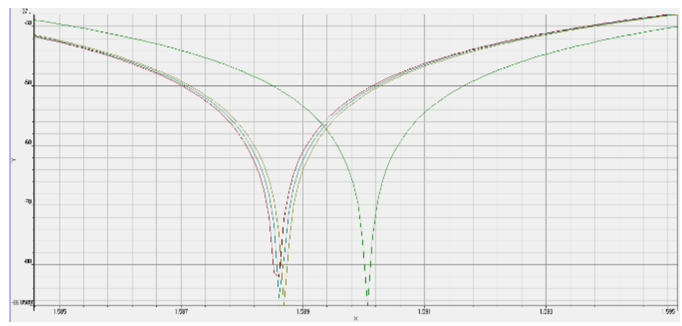

Fig. 7. Power spectrum graph for single waveguide

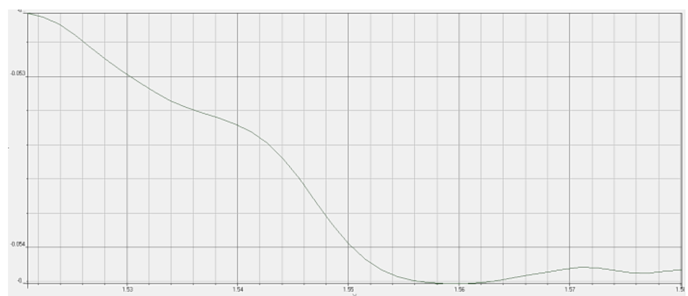

Fig. 8. Power loss

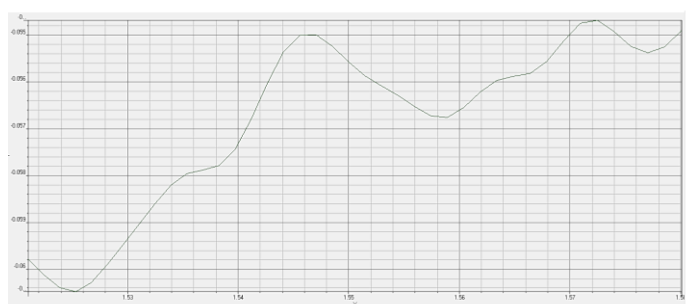

Fig. 9. Power spectrum graph for double waveguide

By monitoring the transmission spectra of a plasmonic ring resonator as the cladding refractive index changes from 1.33 to 1.39 in minute increments, changes in resonance wavelengths may be linked to glucose concentrations. This association makes it possible to employ an optical ring resonator for non-invasive, real-time diabetes diagnosis.

The diagnosis of diabetes mellitus is valid because of the optical ring resonator structure's ability to correctly detect glucose concentrations through minute variations in resonance wavelengths. With the use of this technology, diabetes mellitus may be diagnosed non-invasively and label-free without requiring invasive procedures or blood samples. Furthermore, this approach is novel as it utilizes plasmonic ring resonators, which are ideal for biological sensing applications due to their incredibly sensitive responses to variations in refractive index.

When compared to conventional diabetes detection techniques, the suggested sensor system has a number of benefits. First, it offers real-time glucose monitoring, which enables early illness detection and treatment. Second, because blood collection is non-invasive, there is less chance of infection and the patient feels no discomfort. Furthermore, a trustworthy diagnosis is guaranteed even at low glucose concentrations because to the exceptional sensitivity and specificity of the optical ring resonator construction. All things considered, the suggested sensor system is a promising development in the management of diabetes as it provides patients with a practical and efficient way to check their blood sugar level.

The power coupled at ring's surface, especially the slot region, exhibits a grater notable dip at a specific wavelength. This power is evanescently confined in the Si ridge to a penetration depth definable for the surface plasmon.[29] Scrutinizing the plasmonic ring resonator's transmission spectra across cladding refractive indices from 1.33 to 1.39 (in 0.002 increments) revealed shifting resonance wavelengths. This index range covers those commonly found in biological samples, making the resonator potentially applicable to them [30]. The resonance shifts maintain the alignment of the incident light's propagation constant to that of the excited plasmon, as required for surface plasmon resonance. The consistent red-shifting of the resonances with increasing refractive index demonstrates the ring's sensitivity to surrounding medium changes, underscoring its promise for biological sensing applications [31].

V. Conclusion

Our lab-on-a-chip solution, which is a cost-effective and compact silicon-on-insulator ring resonator biosensor, offers a significant improvement over current techniques. through the waveguide's optimization to link to and excite surface Plasmon polarity. Our water cladding sensor was specially designed to detect even the smallest variations in refractive index, which indicate the amounts of glucose in urine, with extraordinary sensitivity. The sensor's remarkable capability to differentiate between refractive indices 1.335 and 1.339, with a resolution of 0.002, was proven by validation testing. Real-time sensing is made possible by the optimized field confinement in the slot region, which averages 860 nm/RIU. This increases the sensitivity of the sensor. By detecting high urine levels, this biosensor shows potential for a variety of healthcare applications, such as early diabetes diagnosis and the identification of illnesses associated with aberrant glucose metabolism. Our biosensor represents a significant improvement over existing diagnostic standards and practices thanks to its strong performance in a small package. In order to improve accessibility across the board, future work will entail investigating other applications, improving detection parameters, and incorporating the technology into point-of-care devices.

References

[1] J. Al Mahmod, R. Hyder, and Z. Islam, "A Highly Sensitive Metal–Insulator–Metal Ring Resonator-Based Nanophotonic Structure for Biosensing Applications," IEEE Sens. J., vol. 18, no. 16, pp. 6563–6568, 2018.

[2] O. S.Wolfbeis, Springer Series on Chemical Sensors and Biosensors: Method and Applications, vol. 4, 2006.

[3] A. S. Kushwaha, A. Kumar, R. Kumar, and S. K. Srivastava, "Photonics and Nanostructures - Fundamentals and Applications: A study of surface plasmon resonance (SPR) based biosensor with improved sensitivity," Photonics Nanostructures - Fundam. Appl., vol. 31, no. May, pp. 99–106, 2018.

[4] N. Luan, L. Zhao, Y. Lian, and S. Lou, "A High Refractive Index Plasmonic Sensor Based on D-Shaped Photonic Crystal Fiber With Laterally Accessible Hollow-Core Sensor Based on D-Shaped Photonic," IEEE Photonics J., vol. 10, no. 5, pp. 1–7, 2018.

[5] K. A. Tarumaraja, P. S. Menon, S. Shaari, A. G. Ismail, and B. Majlis, "Graphene-Based Plasmonic Photonic Crystal Waveguide Integrated Biosensor Circuit," J. Nanoelectron.

[6] Optoelectron., vol. 13, pp. 839–845, 2018.

[7] X. Sun, D. Dai, L. Thylén, and L. Wosinski, "Double-Slot Hybrid Plasmonic Ring Resonator Used for Optical Sensors and Modulators," Photonics, vol. 2, no. 4, pp. 1116–1130, 2015.

[8] L. Zhou, X. Sun, X. Li, and J. Chen, "Miniature microring resonator sensor based on a hybrid plasmonic waveguide," Sensors, vol. 11, no. 7, pp. 6856–6867, 2011.

[9] J. Melorose, R. Perroy, and S. Careas, Surface Plasmon Nanophotonics, vol. 1, 2015.

[10] L. R. Bard, Allen J.; Faulkner, Fundamentals and Applications Fundamentals and Applications, 2002.

[11] S. Nivedha, P. Ramesh Babu, and K. Senthilnathan, "Surface plasmon resonance: Physics and technology," Curr. Sci., vol. 115, no. 1, pp. 56–63, 2018.

[12] Y. Sun and X. Fan, "Optical ring resonators for biochemical and chemical sensing," Anal Bioanal Chem., 2011; 399:205–11.

[13] P. Schineeweiss, S. Zeiger, T. Hoinkes, A. Rauschenbeutel, and J. Volz, "Fiber ring resonator with a nanofiber section for chiral cavity quantum electrodynamics and multimode strong coupling," Opt Lett., 2017; 42:85–8.

[14] B. E. Little, J. P. Laine, and H. A. Haus, "Analytic theory of coupling from tapered fibers and half-blocks into microsphere resonators," J Lightwave Technol., 1999; 17:704–15.

[15] X. Li, Z. Zhang, S. Qin, M. Qiu, and Y. Su, "Ultra-compact parallel label-free biosensors based on concentric micro-ring resonators in silicon-on-insulator," Asia Optical Fiber Communication and optoelectronic Exposition and Conference, AOE, 2008.

[16] M. Iqbal, M. A. Gleeson, B. Spaugh, F. Tabor, W. G. Gunn, M. Hochberg, T. B. Jones, R. C. Bailey, and C. Gunn, "Label-free biosensor arrays based on silicon ring resonators and high-speed optical scanning instrumentation," IEEE J Sel Top Quantum Electron., 2010; 16:654–61.

[17] A. Abbas, M. J. Linman, and Q. Cheng, "New trends in instrumental design for surface plasmon resonance-based biosensors," Biosens. Bioelectron., vol. 26, no. 5, pp. 1815–1824, 2011

[18] W. Bogaerts, P. De Heyn, T. Van Vaerenbergh, K. De Vos, and S. Kumar, "Silicon microring resonators," vol. 73, no. 1, pp. 47–73, 2012.

[19] P. Sharma, P. Deshmukh, and P. Sharan, "Design and analysis of blood components by using optical sensors," Int. J. Current Res., vol. 5, pp. 2225–2228, Aug. 2013.

[20] A. F. Oskooi, D. Roundy, M. Ibanescu, P. Bermel, J. D. Joannopoulos, and S. G. Johnson, "MEEP: A flexible, free-software package for electromagnetic simulations by the FDTD method," Comput. Phys. Commun., vol. 181, pp. 687–702, Mar. 2010.

[21] K. S. Yee, "Numerical solution of initial boundary value problems involving Maxwell's equations in isotropic media," IEEE Trans. Antennas Propag., vol. 14, no. 3, pp. 302–307, May 1996.

[22] MPB User Tutorial-Ablnitio-MIT. [Online]. Available: http://ab-initio.mit.edu/wiki/index.php/MPB_User_Tutorial, accessed Feb. 15, 2014.

[23] D.Tomky, "Detection, prevention, and treatment of hypoglycemia in the hospital," Diabetes Spectr., vol. 18, no. 1, pp. 39–44, Jan. 2005.

[24] "Hypoglycemia-It's Not All in Your Head, its All in Your Urine." [Online]. Available: http://180degreehealth.com/hypoglycemia, accessed Jul. 17, 2014.

[25] S. Kumari and S. M. Tripathi, "Plasmonic Waveguide Based Optical Ring Resonator For Bio-sensing Application," 2019 Workshop on Recent Advances in Photonics (WRAP), 2019.

[26] P. Sharma and P. Sharan, "Design of Photonic Crystal-Based Biosensor for Detection of Glucose Concentration in Urine," IEEE Sensors Journal, 2015.

[27] R.Annamalai and R. Nedunchelian, Design of optimal bidirectional long short term memory based predictive analysis and severity estimation model for diabetes mellitus, International Journal of Information Technology(IJIT), Vol.15,pages 447-455(2023)

[28] Archana Yadav, et. Al .,Modeling,simulation and computational analysis of plasmonic optical sensor.

[29] g BATiO3 in diabetes mellitus, International Journal of Information Technology(IJIT), Vol.13,pages 2163-2168(2021)

[30] Abid sarwar et.al., Diagnosis of diabetes type-II using hybrid machine learning based ensemble model, International Journal of Information Technology (IJIT), Vol.12pages 419-428(2020).

[31] P.R. Yashaswini et.al., Circular diaphrahm-based MOEMS pressure sensor using ring resonator, International Journal of Information Technology (IJIT), Vol.13 pages 213-220(2021).